Available online at www.sciencedirect.com
ScienceDirect
International Journal of Heat and Mass Transfer 51 (2008) 779–788
International Journal of HEAT and MASS TRANSFER
www.elsevier.com/locate/ijhmt

Conjugate heat transfer in open cavities with a discrete heater at its optimized position

A. Muftuoglu, E. Bilgen *

Ecole Polytechnique Box 6079, Centre Ville, Montreal, QC, Canada H3C 3A7

Received 12 February 2007; received in revised form 21 April 2007
Available online 19 June 2007

Abstract

In this article, we determined optimum position of a discrete heater by maximizing the conductance and then studied heat transfer and volume flow rate with the discrete heater at its optimum position in open cavities. Continuity, Navier–Stokes and energy equations are solved by finite difference-control volume numerical method. The relevant governing parameters were: the Rayleigh numbers from 10^6 to 10^{12}, the Prandtl number, $Pr = 0.7$, the cavity aspect ratio, $A = H/L$ from 0.5 to 2, the wall thickness l/L from 0.05 to 0.15, the heater size h/L from 0.15 to 0.6, and the conductivity ratio k_r from 1 to 50. We found that the global conductance is an increasing function of the Rayleigh number, the conductivity ratio, and a decreasing function of the wall thickness. Best thermal performance is obtained by positioning the discrete heater at off center and slightly closer to the bottom. The Nusselt number and the volume flow rate in and out the open cavity are an increasing function of the Rayleigh number and the wall thickness, and a decreasing function of the conductivity ratio. The Nusselt number is a decreasing function of the cavity aspect ratio and the volume flow rate is an increasing function of it.

Keywords: Conjugate heat transfer; Open cavity; Discrete heat source; Optimum heater position

1. Introduction

The thermal performance of electronic packages containing a number of discrete heat sources has been studied extensively in the literature. The design problem in electronic packages is to maintain cooling of chips in an effective way to prevent overheating and hot spots. This is achieved generally by effective cooling by natural convection, mixed convection and in certain cases by other means such as heat pipes, and finally by better design. In the latter case, the objective is to maximize heat transfer density so that the maximum temperature specified for safe operation of a chip is not exceeded. Thus, optimum placement of discrete heaters may be required with respect to usual equidistant placement. In this respect, few theoretical and experimental studies have been published in various geometries [e.g. [1–7]]. Recently, the authors studied the case of natural convection heat transfer in an open square cavity with one to three heaters placed on the adiabatic wall facing the opening. Their optimum positions were determined and the heat transfer by natural convection was investigated [8]. In these studies, the heaters are placed on an adiabatic wall, yet, in various applications, the discrete heaters are placed on walls with finite thickness and conductance.

In the present study, we will address the case in which the heater is placed on a wall with finite thickness and conductance. Our aim is (i) to determine optimum positions of a discrete heater placed on the vertical wall facing the opening of cavities. The vertical wall has a finite thickness and conductance, and is in contact with the ambient air at both sides. The horizontal walls are insulated and (ii) to study the conjugate heat transfer and determine the thermal performance of the system with the heater at its optimum position.

* Corresponding author. Tel.: +1 514 340 4711x4579; fax: +1 514 340 5917.
E-mail address: bilgen@polymtl.ca (E. Bilgen).

0017-9310/$ - see front matter © 2007 Elsevier Ltd. All rights reserved.
doi:10.1016/j.ijheatmasstransfer.2007.04.017

Nomenclature

A	enclosure aspect ratio $= H/L$
c_p	heat capacity (J/kg K)
g	acceleration due to gravity (m/s)
H	cavity height (m)
h	heater size (m)
k	thermal conductivity (W/m K)
L	cavity width (m)
l	wall thickness (m)
Nu	Nusselt Number, defined by Eq. (6)
p	pressure (Pa)
P	dimensionless pressure $= (p - p_\infty)L^2/\rho\alpha^2$
Pr	Prandtl number $= \upsilon/\alpha$
q''	heat flux (W/m^2)
q	dimensionless heat flux $= \frac{\partial\theta}{\partial X}$
Ra	Rayleigh number $= g\beta q'' L^4/(\upsilon\alpha k)$
t	time (s)
U, V	dimensionless fluid velocities $= uL/\alpha, vL/\alpha$
$\dot{V}$	dimensionless volume flow rate through the opening
X, Y	dimensionless Cartesian coordinates $= x/L, y/L$,
x, y	Cartesian coordinates

Greek symbols

α	thermal diffusivity (m^2/s)
β	volumetric coefficient of thermal expansion $1/K$
υ	kinematic viscosity (m^2/s)
ρ	fluid density (kg/m^3)
ψ	stream function
θ	dimensionless temperature $= (T - T_\infty)/(Lq''/k)$
τ	dimensionless time $= \alpha t/L^2$

Superscript

–	average

Subscripts

ext	extremum
in	into cavity
max	maximum
opt	optimum
out	out of the cavity
∞	ambient value

2. Problem and mathematical model

First, we determine the optimum position of a discrete heating element in open cavities installed on a conducting wall facing the opening, cooled by natural convection. Second, we study heat transfer performance of each case using the heater at its optimum position and carry out a sensitivity study on the governing parameters.

Schematic of the two-dimensional open square cavity with a discrete heating element and the boundary conditions are shown in Fig. 1. Horizontal boundaries of the cavity are adiabatic, the left face of the solid wall is isothermal and its right side is in the open cavity in contact with the ambient air. A discrete heating element is installed on the solid wall inside the cavity. The heating element of height h and coordinate $(0, y_i)$ dissipates heat at constant heat flux, q''. The cooling air from a reservoir enters the cavity through the lower part of the opening; it circulates along the heating element and exits from the upper part of the opening.

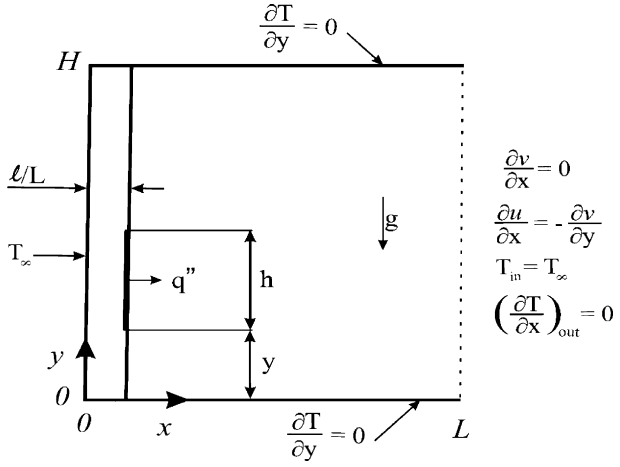

Fig. 1. Schematic of open cavities, the coordinate system and boundary conditions.

We assume that the fluid is Newtonian, the radiation is negligible and the third-dimension has a negligible effect on the flow and heat transfer. With these assumptions, we use two-dimensional conservation equations for mass, momentum and energy with Bussinesq approximation. By using L as the length scale, α/L as the velocity scale, Lq''/k as the temperature scale and L^2/α for the time scale, we obtain following non-dimensional equations

$$\frac{\partial U}{\partial X} + \frac{\partial V}{\partial Y} = 0 \tag{1}$$

$$\frac{\partial U}{\partial \tau} + U\frac{\partial U}{\partial X} + V\frac{\partial U}{\partial Y} = -\frac{\partial P}{\partial X} + \Gamma Pr\nabla^2 U \tag{2}$$

$$\frac{\partial V}{\partial \tau} + U\frac{\partial V}{\partial Y} + V\frac{\partial V}{\partial Y} = -\frac{\partial P}{\partial Y} + \Gamma Pr\nabla^2 V + RaPr\theta \tag{3}$$

$$\frac{\partial \theta}{\partial \tau} + U\frac{\partial \theta}{\partial X} + V\frac{\partial \theta}{\partial Y} = k_r\nabla^2\theta \tag{4}$$

where Γ is a general diffusion coefficient and 1 in the fluid region and 10^{15} in the solid region, k_r is 1 in the fluid region and k_s/k_f in the solid region. Γ and k_r are introduced in the equations to ensure $U = V = 0$ everywhere including at the solid–fluid interface and the conduction is accounted for in the solid region.

The governing parameters are $Ra = g\beta q'' L^4/(\upsilon\alpha k)$ and $Pr = \upsilon/\alpha$.

The average and normalized Nusselt numbers are calculated as

$$\overline{Nu} = \frac{-\int_0^A \frac{\partial\theta}{\partial X}\,dY}{\int_0^A (\theta_1 - \theta_2)} \tag{5}$$

$$Nu = \frac{\overline{Nu}_{Ra}}{\overline{Nu}_{Ra=0}} \tag{6}$$

The volume flow rate, $\dot{V}$ is calculated as

$$\dot{V} = -\int_{X=1} U_{\text{in}}\,dY \tag{7}$$

where $U_{\text{in}} = U_{X=1}$ if $U_{X=1} < 0$ and $U_{\text{in}} = 0$ if $U_{X=1} \geqslant 0$.

The stream function is calculated from its definition as

$$U = -\frac{\partial\psi}{\partial Y}, \quad V = \frac{\partial\psi}{\partial X} \tag{8}$$

ψ is zero on the solid surfaces and the streamlines are drawn by $\Delta\psi = (\psi_{\max} - \psi_{\min})/n$ with n is the number of increments.

Boundary conditions are

$$\text{On solid surfaces: } U = 0,\ V = 0 \tag{9}$$

$$X = 0 \text{ to } 1,\ Y = 0 \text{ and } A:\ \frac{\partial\theta}{\partial n} = 0 \tag{10}$$

$$X = 0,\ Y = 0 \text{ to } A: \theta = 0 \tag{11}$$

$$X = 1,\ Y = 0 \text{ to } A:\ \frac{\partial V}{\partial X} = 0, \quad \frac{\partial U}{\partial X} = -\frac{\partial V}{\partial Y}, \quad \left(\frac{\partial\theta}{\partial X}\right)_{\text{out}} = 0, \quad \theta_{\text{in}} = 0 \tag{12}$$

$$\text{On the heater: } q = \frac{\partial\theta}{\partial X} \tag{13}$$

The boundary condition at the opening, Eq. (12) is shown to be a satisfactory for the case of computation domain confined to the open cavity [9].

The conductance is calculated as

$$C = \frac{\int_y^{y+h} q''\,dy}{k(T_{\max} - T_\infty)} = \frac{h/L}{\theta_{\max}} \tag{14}$$

3. Numerical technique

The numerical method used to solve Eqs. (1)–(4) with the boundary conditions Eqs. (9)–(13) is the SIMPLER (semi-implicit method for pressure linked equations revised) algorithm [10]. The computer code based on the mathematical formulation presented above and the SIMPLER method were validated earlier with respect to the benchmark [11]. The results of validation with the benchmark [12] as well as another [13] showed that the deviations in Nusselt number and the maximum stream function at $Ra = 10^6$ were 0.60% and 1.12%, respectively. It was seen that the concordance was excellent. In addition, the average Nusselt numbers at the hot and cold walls were compared, which showed a maximum difference of about 0.5% in all runs. The present code was tested also to simulate the case studied by Chan and Tien with enlarged computational domain [14]. We used restricted computational domain and compared the results with theirs with extended computational domain. For $Ra = 10^6$ for example, we found that the deviations in the Nusselt number and the volume flow rate were 1.53% and 0.59%, respectively, which is considered to be satisfactory [9].

Table 1
Grid independence study results with $A = 1$, $\ell/L = 0.10$, $k_r = 10$

Size		21×21	31×31	61×61	101×101
$Ra = 10^8$	Nu	3.227	3.111	3.103	3.077
	V	5.855	5.557	5.567	5.455
	C	3521.540	3546.938	3582.945	3597.985
$Ra = 10^{10}$	Nu	13.159	12.140	12.069	11.775
	V	24.382	29.913	29.743	29.256
	C	4125.980	3964.059	3953.611	3953.611

Uniform grid in X and Y direction was used for all computations. Grid convergence was studied for the case of square cavity having $\ell/L = 0.10$ and $k_r = 10$ with grid sizes from 21×21 to 101×101 at $Ra = 10^8$ and 10^{10}. The results are presented in Table 1. We see, for example, at $Ra = 10^{10}$ that between 31×31 and 61×61, the variation in Nusselt is 0.59%, it is 0.57% in volume flow rate, and 0.28% in conductance. Thus, 31×31 grid size was a good choice from the computation time and precision point of view for the square cavity. We conducted similar tests with the shallow and tall cavities and used 61×31 for $A = 0.5$ and 31×61 for $A = 2$ grid sizes. The grid size in the wall was 5, 10 and 15 in the X direction for the wall thickness of $\ell/L = 0.05$, 0.10 and 0.15, respectively, and the rest were in the cavity. Using a computer with a processor of 3.2 GHz clock speed, for $A = 1$, with 31×31 grid size, at $Ra = 10^{10}$, the typical execution time was 92 s.

A converged steady state solution was obtained by iterating in time until variations in the primitive variables between subsequent time steps were:

$$\sum(\phi_{i,j}^{\text{old}} - \phi_{i,j}) < 10^{-4} \tag{15}$$

where ϕ stands for U, V, and θ.

Within the same time step, the residual of the pressure term was less than 10^{-3} [10]. In addition, the accuracy of the solution was double-checked using the energy conservation on the domain to ensure it was less than 10^{-4}.

4. Results and discussion

In the first part, we present the optimization study results and in the second, a parametric study results obtained with the discrete heating elements at their optimum position. The variable geometrical parameters considered are, the aspect ratio, $A = 0.5, 1$ and 2, and the dimensionless wall thickness, $\ell/L = 0.05$, 0.10 and 0.15. The dimensionless height of heating element was set as

$h/L = 0.15$, 0.3 and 0.6 corresponding to $A = 0.5$, 1 and 2, respectively, which results in a constant ratio of the heater to cavity height. The Rayleigh number was varied from $Ra = 10^6$ to 10^{12}. The Prandtl number, $Pr = 0.70$ for air was kept constant. The conductivity ratio was varied from $k_r = 1$ to 50.

4.1. Optimization study

We carried out studies to obtain the optimum position of the heating element by varying its position. The procedure was as follows: (i) We compute conductance $C(Y)$ at a constant Ra, (ii) we determine the maximum conduction, C_{max} at its optimum position Y_{opt}. We note that Y_{opt} in this study shows the lower edge position of the heater, yet C_{max} may be somewhat near the center of the heater. (iii) We repeat the steps (i) and (ii) to determine $C(Y)$, C_{max} and Y_{opt} at all the other Rayleigh numbers, from 10^6 to 10^{12}.

Typical results to obtain the conductance $C(Y)$ for the case of $\ell/L = 0.10$, $h/L = 0.30$, $A = 1$ and $k_r = 10$ at $Ra = 10^6$, 10^8 and 10^{10} are presented in Fig. 2a. We can make the following observations: (i) for all the Rayleigh numbers, the conductance changes with the position of the heater. We have smaller conductance at the lowest position when the heater is at the bottom; the conductance is increasing rapidly as its position is raised reaching a broad maximum around $0.15 < Y < 0.55$ and it is decreasing thereafter to another low conductance at the top position. For example, at $Ra = 10^6$, the maximum is when the lower edge of the heater is $Y_{opt} = 0.30$, which corresponds to the position of heater Y from 0.30 to 0.60. The center of the heater is at $Y = 0.45$ for this case. This result is expected since the heat transfer regime at $Ra = 10^6$ is conduction dominated and the heater's optimum position is slightly off center at a lower position of the cavity, (ii) as the Rayleigh number is increased, the air flow as well as the conductance is increased. As we will see later, the heat transfer becomes by convection as well as conduction at $Ra = 10^8$, the heater position is again at the same level, at $Y_{opt} = 0.30$. For $Ra = 10^{10}$, it is at $Y_{opt} = 0.40$. Following the increased air flow rate, the conductance, $C(Y)$ is increased accordingly, (iii) for all cases, we see broad maxima; we note that using the computation results or changing scale of conductance, it is not difficult to identify C_{max} at its Y_{opt}.

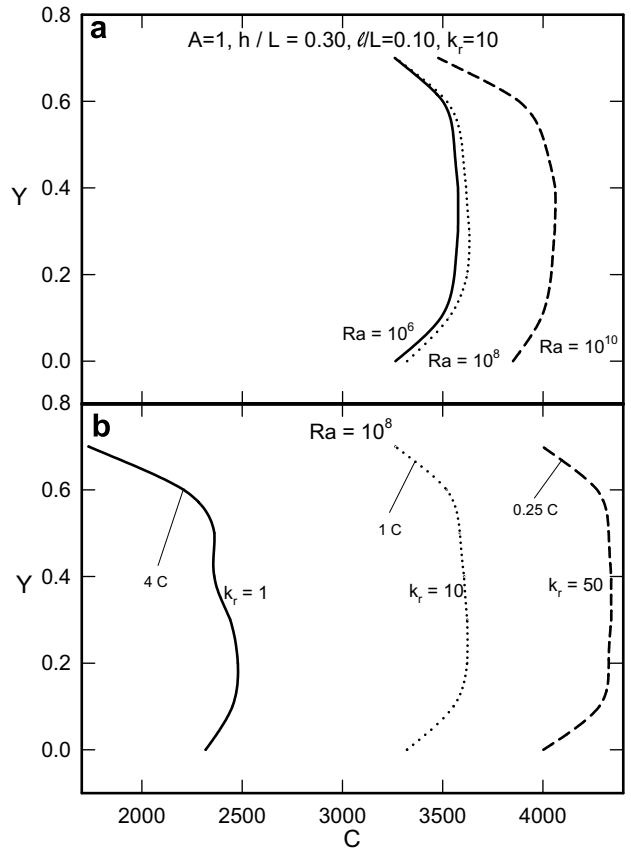

Fig. 2. The maximization of the global conductance with the heat source of $h/L = 0.30$. The scales of the curves for $k_r = 1$ and 50 are $4C$ and $0.25C$ = abscissa value, respectively.

The effect of the conductivity ratio, k_r at $Ra = 10^8$ is presented in Fig. 2b for the same case in Fig. 2a. We see that the conductance is strongly affected by the conductivity ratio. Higher is the conductivity ratio, higher becomes the conductance. As the conductivity ratio is increased, ψ_{ext}/θ_{max} are both reduced since the heat transfer in the cavity is reduced for a given Rayleigh number. For example at $Ra = 10^8$, for $k_r = 1$, $\psi_{ext}/\theta_{max} = -12.8222/484.22E\text{-}6$, for $k_r = 10$, $\psi_{ext}/\theta_{max} = -5.55695/82.82E\text{-}6$ and for $k_r = 50$, $\psi_{ext}/\theta_{max} = -1.98097/17.32E\text{-}6$. We see that both $\psi_{ext}/\theta_{max} =$ are decreasing function of k_r. The optimum positions are $Y = 0.2$ for $k_r = 1, 0.3$ for $k_r = 10$ and 50.

To see the reason for the observations made with Fig. 2, we present streamlines and isotherms in Fig. 3 for the cases corresponding to Fig. 2 at $Ra = 10^6$, 10^8 and 10^{10} (shown with a–c, respectively) and $k_r = 1$ (the upper figure) and 10 (the lower figure) for each Rayleigh number. The heater size is $h/L = 0.30$ and it is at its optimum position for each Rayleigh and conductivity ratio. We observe in Fig. 3a at $Ra = 10^6$ that the heat transfer is convective for $k_r = 1$; it is conduction dominated for $k_r = 10$. This is expected since for $k_r = 1$, the wall having the same conductivity as that of the air, is insulated. Thus, the heat dissipated by the heater is mostly transferred by convection in the cavity. For $k_r = 10$, a part of the heat goes through the wall and dissipated at the left side at $\theta = 0$ and the rest is transferred by convection through the cavity opening. Indeed, for $k_r = 1$, $\psi_{ext}/\theta_{max} = -1.0091893/632.9E\text{-}6$, and for $k_r = 10$, $-0.1262171/83.9E\text{-}6$, which show highly increased convection and reduced maximum temperature for $k_r = 1$. At $Ra = 10^8$ in Fig. 3b, for $k_r = 1$, $\psi_{ext}/\theta_{max} = -12.8222/484.22E\text{-}6$, and for $k_r = 10$, $-5.55695/82.82E\text{-}6$. We see in this case a similar phenomenon to that at $Ra = 10^6$, however the convection becomes strong also with $k_r = 10$. Finally, at $Ra = 10^{10}$ in Fig. 3c, for $k_r = 1$, $\psi_{ext}/\theta_{max} = -39.141833/290.03E\text{-}6$, and for $k_r = 10$, $-27.326857/74.07E\text{-}6$, thus, the heat transfer is mainly by convection

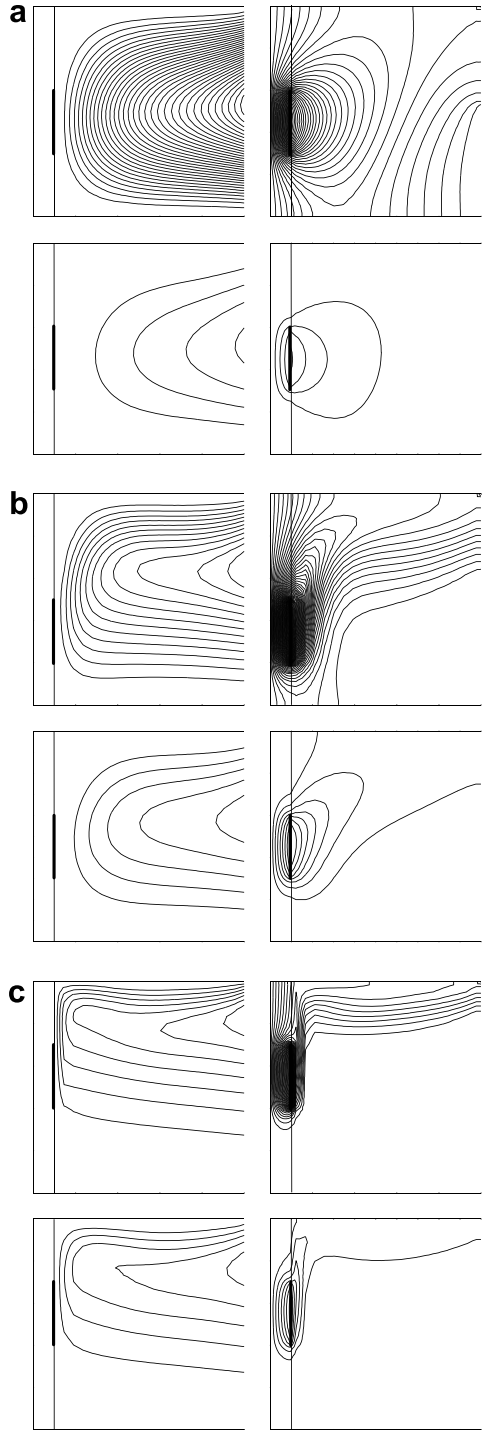

Fig. 3. Streamlines (on the left) and isotherms (on the right) for $A = 1$, $\ell/L = 0.10$, for (a) $Ra = 10^6$, (b) $Ra = 10^8$ and (c) $Ra = 10^{10}$. The upper figure is for $k_r = 1$ and the lower figure is for $k_r = 10$ for each case.

for both. Following our observations with Fig. 2a, we see for $k_r = 0.10$ at the three Rayleigh numbers of Fig. 3 that there is no change in the circulation of air in the cavity at $Ra = 10^6$ and 10^8, hence the heater position is the same. At $Ra = 10^{10}$, the air circulation shifts upward and the heater position becomes higher. At $Ra = 10^8$ and for $k_r = 1$ and 10 of Fig. 2b, again we see in Fig. 3b that the air circulation is relatively strong and sweeps lower level of the wall for

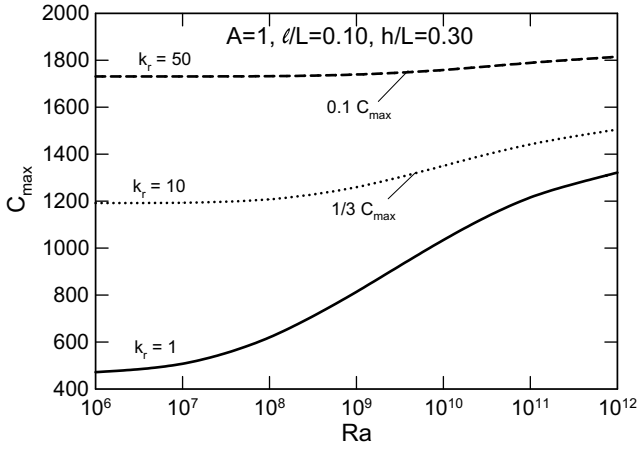

Fig. 4. Maximum conductance as a function of the Rayleigh number with the conductivity ratio as a parameter. The scales of the curves for $k_r = 10$ and 50 are (1/3) C_{max} and $0.1C_{max}$ = ordinate value, respectively.

$k_r = 1$. The heater position is at $Y_{opt} = 0.20$. In contrast, the air circulation is weaker and at higher level for $k_r = 10$, hence the heater position is at $Y_{opt} = 0.30$. Figs. 2 and 3 show that the other parameters being constant, the optimum heater position is a strong function of the Rayleigh number as well as the conductivity ratio.

It was seen for the majority of the cases studied (not shown here) that the optimum heater positions Y_{opt} deter-

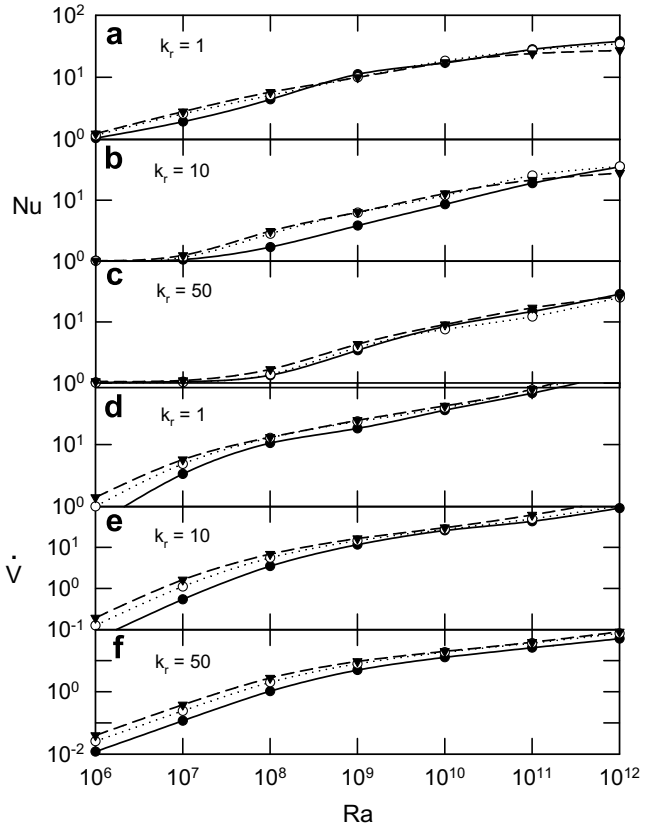

Fig. 5. Nusselt number (a–c) and volume flow rate (d–f) as a function of Rayleigh number for $A = 1$ with ℓ/L and k_r as parameters. Solid line: $\ell/L = 0.05$, dotted line: $\ell/L = 0.10$, dashed line: $\ell/L = 0.15$.

mined from the computed data were generally slightly decreasing function of the Rayleigh number, although in some cases, as observed in Fig. 3 for example, it was slightly increasing function. On the other hand, in most of the cases, Y_{opt} is found to be an increasing function of the conductivity ratio as observed earlier with Fig. 2. The maximum conductance, C_{max} obtained from the computed data showed for all cases that C_{max} is an increasing function of both Ra and k_r. For example, we present in Fig. 4, C_{max} as a function of Ra with k_r as a parameter for the case of $A = 1$, $h/L = 0.30$ and $k_r = 1, 10$ and 50. We see that C_{max} is an increasing function of both Ra and k_r. This dependence is stronger when the conductivity ratio is small. This is because, as we discussed earlier, $k_r = 1$ corresponds to insulated wall case, in which the cooling is mainly by convection. As a result, θ_{max} is higher and by Eq. (14), C_{max} lower. For higher k_r, the cooling is by conduction through the wall and by convection in the cavity, hence the cooling is better, θ_{max} is smaller and C_{max} is higher.

4.2. Heat transfer and volume flow rate

The average normalized Nusselt number by Eq. (6) and the volume flow rate $\dot{V}$ by Eq. (7) are calculated as a function of Rayleigh number and presented in Fig. 5 for the case of $A = 1$ with ℓ/L and k_r as parameters.

For $k_r = 1$, we see in Fig. 5a that Nu is an increasing function of Ra and ℓ/L. Starting at $Ra = 10^6$, the heat transfer is by convection dominated. The Nusselt number is a weak function of the wall thickness since for $k_r = 1$, the wall is insulated and ℓ/L has a minor effect on the wall conductance. Nevertheless, we see that for $\ell/L = 0.05$ with respect to $\ell/L = 0.10$ and 0.15, the conductance through the wall is relatively higher, i.e. the heat transfer by conduction is higher as a consequence of which convection is lower in the cavity at Ra from 10^6 to 10^8. Indeed, as the wall thickness is increased the conductance becomes smaller, the heat transfer by conduction through the wall is lower, and the convection heat transfer in the cavity becomes dominant. At $Ra > 10^8$ the effect of ℓ/L on Nu is less. For $k_r = 10$, Fig. 5b shows a similar result, i.e. for $\ell/L = 0.05$ and 10 the convection starts at $Ra > 10^7$ above which it becomes dominant. The effect of ℓ/L on Nu is considerable: at $Ra > 10^7$, for $\ell/L = 0.05$, the wall conductance is relatively high, as a result of which Nu is relatively lower with respect to $\ell/L = 0.10$ and 0.15. For $k_r = 50$ in Fig. 5c, the heat transfer is conduction dominated up to $Ra = 10^8$ above which the convection is the main heat transfer mode and the wall thickness ℓ/L has a relatively smaller effect on Nu. This is for the same reason as discussed above with

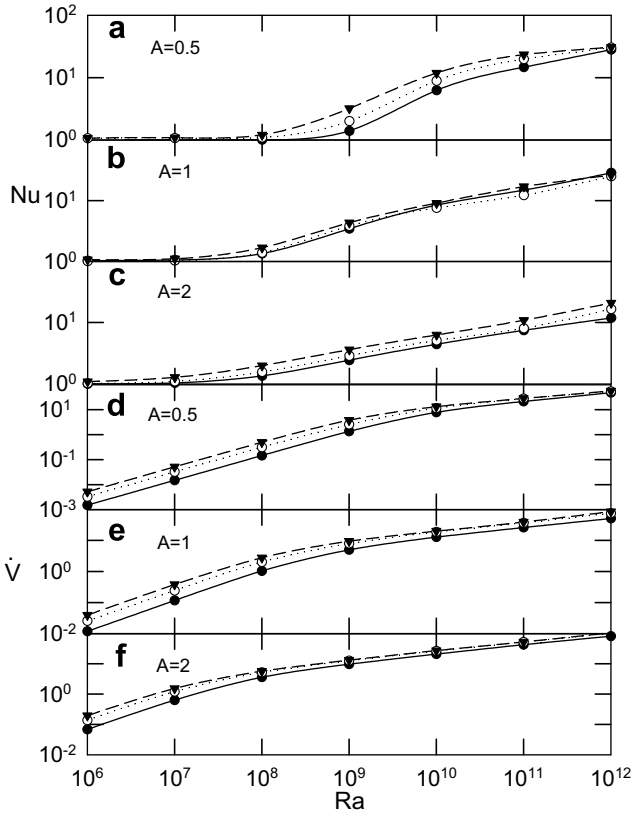

Fig. 6. Nusselt number (a–c) and volume flow rate (d–f) as a function of Rayleigh number for $k_r = 50$, $h/L = 0.15$ for $A = 0.5$, $h/L = 0.30$ for $A = 1$ and $h/L = 0.60$ for $A = 2$ with ℓ/L and A as parameters. Solid line: $\ell/L = 0.05$, dotted line: $\ell/L = 0.10$, dashed line: $\ell/L = 0.15$.

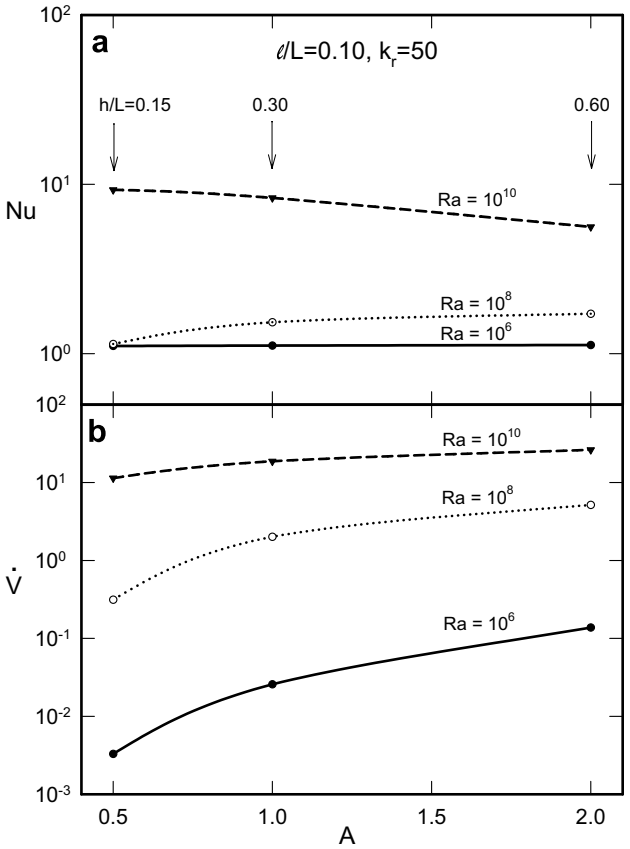

Fig. 7. Nusselt number (a) and volume flow rate (b) as a function of the aspect ratio at various Rayleigh numbers.

Fig. 5a. Thus, the heat transfer by conduction through the wall is increasing with increasing k_r as a consequence of which the heat transfer by convection in the cavity is relatively weaker. Generally, Nu is an increasing function of Ra, except at conduction dominated regime as observed in Fig. 5a–c.

The volume flow rate as a function Rayleigh number with k_r and ℓ/L as parameters is presented in Fig. 5d–f. Following the results in Fig. 5a–c, we observe that $\dot{V}$ is an increasing function of Ra and ℓ/L and decreasing function of k_r. At low Ra, since $\dot{V}$ is smaller, the difference for various ℓ/L is more discernable. Further, $\dot{V}$ is smaller for increasing k_r and decreasing ℓ/L. The same is true at higher Ra however due to logarithmic scale, they are less discernible.

We present Nu and $\dot{V}$ as a function of Ra with the cavity aspect ratio, A and ℓ/L as parameters in Fig. 6a–f. The other parameters are $k_r = 50$ and $h/L = 0.15$ for $A = 0.05$, $h/L = 0.30$ for $A = 1$ and $h/L = 0.60$ for $A = 0.60$. For $A = 0.5$, i.e. the shallow cavity, the heat transfer regime is by conduction at Ra from 10^6 to 10^8, even beyond for $\ell/L = 0.05$, thereafter it is convection dominated. Nu is

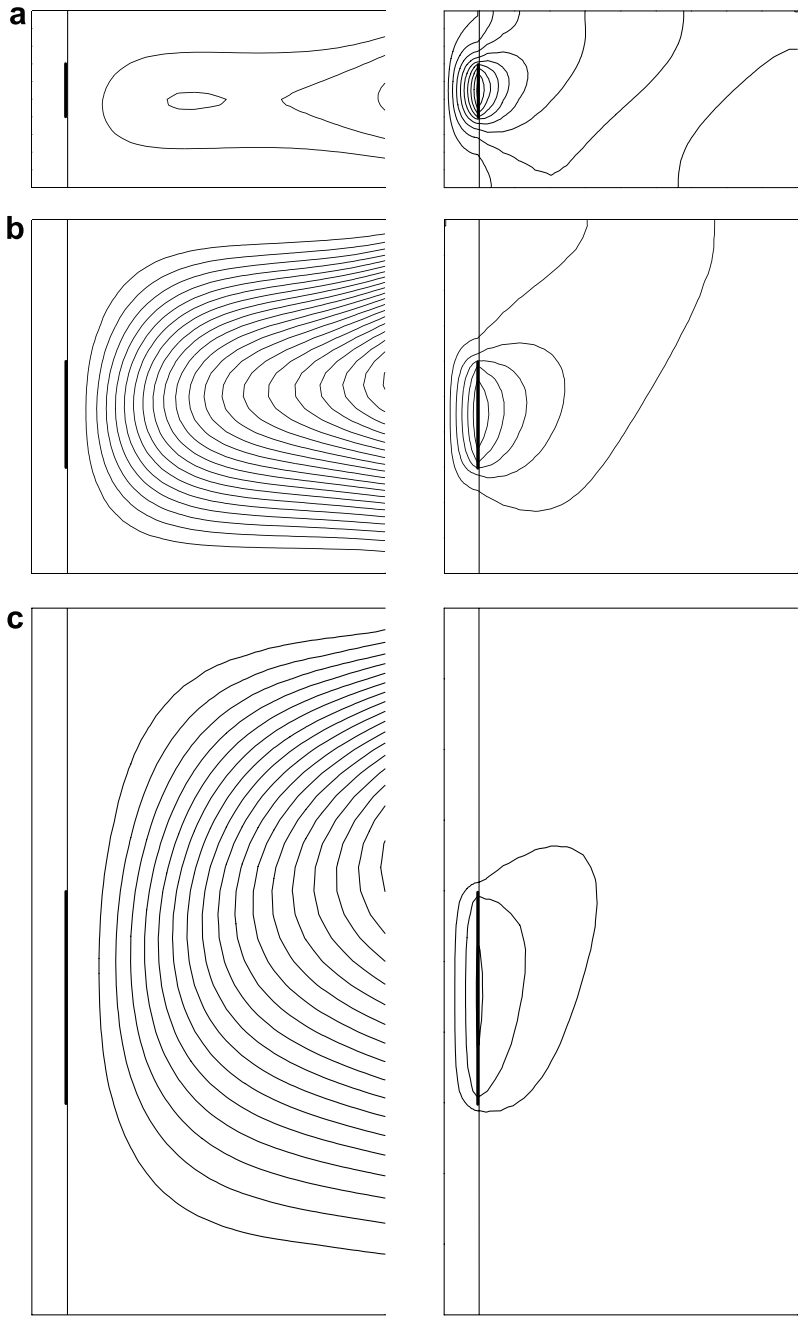

Fig. 8. Streamlines (on the left) and isotherms (on the right) for the case of Fig. 7 ($\ell/L = 0.10$, $k_r = 50$) and $Ra = 10^8$. (a) $A = 0.5$, $h/L = 0.15$, (b) $A = 1$, $h/L = 0.30$, and (c) $A = 2$, $h/L = 0.60$.

an increasing function of Ra and ℓ/L. As the cavity aspect ratio, A increases, the convection starts to be dominant regime at lower Ra numbers: for $A = 1$, i.e. square cavity, the convection starts at $Ra > 10^7$, and for $A = 2$, i.e. the tall cavity, it starts at $Ra > 10^6$. Nu is a weak function of ℓ/L for $A = 1$, and it is a strong function of it for $A = 2$. We see that for all cases of the cavity aspect ratio, Nu and $\dot{V}$ are an increasing function of Ra and ℓ/L.

The flow rate, $\dot{V}$ as a function of Ra with ℓ/L as a parameter is shown in Fig. 6d–f. We see that $\dot{V}$ is an increasing function of both Ra and ℓ/L for $A = 0.5$, 1 and 2. These results expected following our observations in Fig. 6a–c. Generally, the flow rate is reduced with decreasing cavity aspect ratio, A.

Next, we will present the effects of the aspect ratio, A, the conductivity ratio, k_r and the wall thickness, ℓ/L on the Nusselt number and the volume flow rate.

Fig. 7 shows Nu and $\dot{V}$ as a function of A with Ra as a parameter while keeping $\ell/L = 0.10$ and $k_r = 50$ constant. The heater length, h/L is variable with different aspect ratio, A, which is shown in the figure. It is noted that $k_r = 50$ corresponds to the case with high conductance through the wall, as a result, relatively less convection in the cavity. We see in Fig. 7a that at low Rayleigh number, $Ra = 10^6$, the heat transfer is conduction dominated, and $Nu \cong 1$ and almost the same for shallow, square and tall cavities. At $Ra = 10^8$ and $A = 0.5$, i.e. a shallow cavity, the heat transfer is still conduction dominated; however, for square and tall cavities, the convection is significant. The reason for the increased convection heat transfer at higher aspect ratios is due to increased flow through the relatively larger opening. Indeed, $\psi_{ext} = -0.316515$ for $A = 0.5$ and $\psi_{ext} = -5.16181$ for $A = 2$, thus showing the circulation is increased by 16 times. In contrast, Nu is increased by less than 1.5 times. At $Ra = 10^{10}$, the heat transfer is convection dominated in all cases; Nu became a decreasing function of the aspect ratio. $\psi_{ext} = -11.4165$ and -26.2306 for $A = 0.5$ and 2, respectively, i.e. the circulation is increased by 2.3 times. Thus, the cooling is done by circulating more air through the cavity, as we will see next with Fig. 8, the maximum temperature is decreased, as a result of which Nu is decreased by 1.8 times. At still higher Rayleigh number, $Ra = 10^{12}$ (not shown in Fig. 7), the Nusselt number was similarly a decreasing function of A. Fig. 7b shows $\dot{V}$ as a function of A for the same case; $\dot{V}$ is increasing with A from 0.5 to 2 at all Rayleigh numbers. At $Ra = 10^{10}$ for example, $\dot{V}$ is increased by 1.64 times when the aspect ratio, A changed from 0.5 to 1 and 1.4 times when it is changed from 1 to 2. The results show that the volume flow rate increases due to more efficient

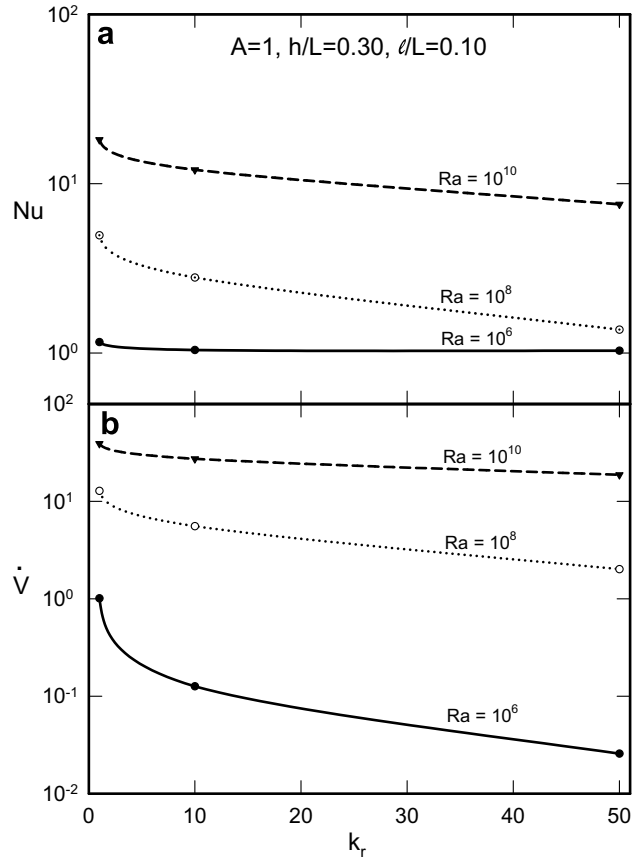

Fig. 9. (a) Nusselt number and (b) flow rate as a function of the conductivity ratio with the Rayleigh number as a parameter.

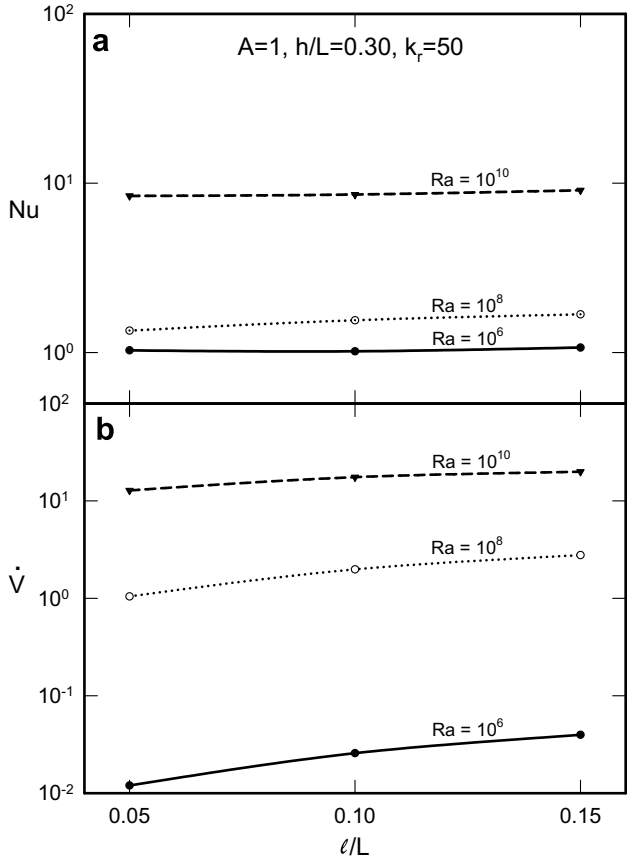

Fig. 10. Nusselt number (a) and volume flow rate (b) as a function of the wall thickness with the Rayleigh number as a parameter.

circulation through larger openings, like tall cavity. The flow rate $\dot{V}$ is a strong function of A at low Ra; it is less so as Ra increases. In fact, $\dot{V}$ for A from 0.5 to 2 increases about 42 times at $Ra = 10^6$ and about 1.8 times at $Ra = 10^{12}$.

To see the reason for changes in the volume flow rate and heat transfer with cavity aspect ratio, the streamlines and isotherms for the same case of Fig. 7 at $Ra = 10^8$ are traced and presented in Fig. 8 for $A = 0.5, 1$ and 2. ψ_{ext}/θ_{max} for $A = 0.5, 1$ and 2 in Fig. 8a–c are −0.316515/27.76E-6, −2.01127/17.33E-6 and −5.16181/9.36E-6, respectively. The streamlines and isotherms show that the flow in the shallow cavity is weak and the maximum temperature is high; in contrast, in the square cavity, the circulation intensity is increased by 15% and the maximum temperature is reduced by 36%. For the tall cavity, the circulation intensity is increased further by 157% and the maximum temperature is decreased by 50%. We see that the aspect ratio is a strong parameter affecting the maximum temperature and as a result the heat transfer as observed with Fig. 7.

The effect of k_r on Nu and $\dot{V}$ for the case of $A = 1$, $h/L = 0.30$ and $\ell/L = 0.10$ is presented in Fig. 9 at $Ra = 10^6$, 10^8 and 10^{10}. We see that both Nu and $\dot{V}$ are decreasing function of k_r at all three Rayleigh numbers. At $Ra = 10^6$, the heat transfer is conduction dominated and it is less dependent on k_r. At higher Rayleigh numbers, following earlier observations with Figs. 5 and 6, the results are: as k_r is increased, the conductance is increased, as a result of which the heat transfer and the volume flow rate in the cavity are decreased. We see that k_r is a strong parameter affecting the heat transfer and flow rate in the cavity.

The effect of the wall thickness, ℓ/L on Nu and $\dot{V}$ for the same case of Fig. 9, but with $k_r = 50$ is presented in Fig. 10 at the same three Rayleigh numbers. Generally, Nu and $\dot{V}$ are an increasing function of ℓ/L, except for Nu at $Ra = 10^6$. As the wall thickness is increased, the conductance through the wall is decreased; as a result, the heat transfer and the volume flow rate are increased through the open cavity. However, we see that the effect of the wall thickness at high Rayleigh numbers is not too significant.

5. Conclusions

We studied natural convection heat transfer in open cavities with a discrete heat source installed at its optimum position at the vertical wall with finite thickness facing the opening. The aspect ratio was varied from 0.5 to 2, the wall thickness from 0.05 to 0.15 and the heater size from 0.15 to 0.60. The Rayleigh number varied from 10^6 to 10^{12}, the conductivity ratio from 1 to 50; the Prandtl number was 0.7. Conservation equations of mass, momentum and energy were solved by finite difference-control volume numerical method. At the beginning, the optimum position of discrete heat source was determined. Then, the heat transfer and volume flow rate were determined. In view of the results presented, the main points can be summarized as follows.

The optimum position of a discrete heater in an open cavity is usually at its off center. Its position depends on the Rayleigh number, the conductivity ratio of the wall, the aspect ratio of the cavity and the wall thickness.

In determining the maximum conductance, we observed broad optima. However, this did not cause any difficulty in determining the position of heaters since numerical results clearly showed the maximum conductance and its coordinates. On the other hand, we note broad optima may give certain flexibility for positioning of the heater if the circumstances require it.

Depending on the cavity aspect ratio and the conductivity ratio, the heat transfer is conduction dominated at low Rayleigh numbers, Ra from 10^6 to 10^8; it is convection dominated regime at higher Rayleigh numbers up to 10^{12} in this study. Generally, the Nusselt number and the volume flow rate are increasing functions of the Rayleigh number and the wall thickness. The Rayleigh number is a decreasing function of the cavity aspect ratio and the conductivity ratio. The volume flow rate is an increasing function of the cavity aspect ratio and a decreasing function of the conductivity ratio. Ra, A, k_r are significant and ℓ/L is relatively less significant parameters affecting thermal performance of discrete heaters at their optimum positions.

Acknowledgements

The financial support for this study by Natural Sciences and Engineering Research Council Canada is acknowledged.

References

[1] H.Y. Wang, F. Penot, J.B. Saulnier, Numerical study of a buoyancy-induced flow along a vertical plate with discretely heated integrated circuit packages, Int. J. Heat Mass Transfer 40 (1997) 1509–1520.
[2] Y. liu, N. Phan-Tien, An optimum spacing problem for three chips mounted on a vertical substrate in an enclosure, Numer. Heat Transfer A 37 (2000) 613–630.
[3] A.K. da Silva, S. Lorente, A. Bejan, Optimal distribution of discrete heat sources on a wall with natural convection, Int. J. Heat Mass Transfer 47 (2004) 203–214.
[4] A.K. da Silva, S. Lorente, A. Bejan, Optimal distribution of discrete heat sources on a plate with laminar forced convection, Int. J. Heat Mass Transfer 47 (2004) 2139–2148.
[5] A.K. da Silva, S. Lorente, A. Bejan, Maximal heat transfer density in vertical morphing channels with natural convection, Numer. Heat Transfer A 45 (2004) 135–152.
[6] A.K. da Silva, G. Lorenzini, A. Bejan, Distribution of heat sources in vertical open channels with natural convection, Int. J. Heat Mass Transfer 48 (2005) 1462–1469.
[7] A.K. da Silva, L. Gosselin, Optimal geometry of L and C-shaped channels for maximum heat transfer in natural convection, Int. J. Heat Mass Transfer 48 (2005) 609–620.
[8] A. Muftuoglu, E. Bilgen, Natural convection in an open square cavity with discrete heaters at their optimized positions. J. Thermal. Sci., in press, doi:10.1016/j.ijthermalsci.2007.04.002.
[9] O. Polat, E. Bilgen, Conjugate heat transfer in inclined open shallow cavities, Int. J. Heat Mass Transfer 46 (2003) 1563–1573.

[10] S.V. Patankar, Numerical Heat Transfer and Fluid Flow, Hemisphere Publishing Corporation, New York, 1980.
[11] E. Bilgen, R. Ben Yedder, Natural convection in enclosure with heating and cooling with sinusoidal temperatures on one side, Int. J. Heat Mass Transfer 50 (2007) 139–150.
[12] D. de Vahl Davis, Natural convection of air in a square cavity: a benchmark solution, Int. J. Numer. Meth. Fluid 3 (1983) 249–264.
[13] D.C. Wan, B.S.V. Patnaik, G.W. Wei, A new benchmark quality solution for the buoyancy driven cavity by discrete singular convolution, Numer. Heat Transfer B 40 (2001) 199–228.
[14] Y.L. Chan, C.L. Tien, A numerical study of two-dimensional natural convection in square open cavities, Numer. Heat Transfer 8 (1985) 65–80.